



## Reservoir Characterisation Using Seismic Inversion Techniques for Mapping of Prospects

Samuel T. Ebong<sup>\*</sup>; Aniekam M. Ekanem and Nyakno J. George

Received: December 10, 2022 / Accepted: January 23, 2023

© REJOST 2023

### Abstract

Reservoir Characterization using integrated 3-D seismic and well log data of M oil field, Niger Delta, was carried out with the aim of identifying reservoir rocks from qualitative interpretation of subsurface seismic view of M oil field through rock properties and acoustic impedance inversion analyzed in some selected reservoirs from the oil field. Rock attributes such as Lamé's parameters terms ( $\lambda\rho$  and  $\mu\rho$ ),  $V_p/V_s$ , P - Impedance, S - Impedance from available petrophysical data obtained from the field were discriminated, which better describe the reservoir of interest (M - 5000). Inversion of the post-stack seismic data was also carried out to generate acoustic impedance,  $V_p/V_s$ ,  $I_p$ ,  $I_s$ ,  $\lambda\rho$  and  $\mu\rho$  volumes. Data slices of the inverted acoustic impedance volumes were then generated to observe the locations if along hydrocarbon charged sands, wet sands or shales channels. Three wells (M-1, M-2 and M-3) were analysed and M-5000 was identified as reservoir of interest. Inversion result in M oil

field revealed that the P-wave / Gamma ray curve is bounded by the top of M-5000 on inverted volumes with the lowest values of  $V_p/V_s$  (1.9290),  $I_p$  (18176),  $\lambda\rho$  (6.7), and  $\mu\rho$  (18.68), which indicate hydrocarbon (gas) charged sands. It means that Gas saturation is detected at the depth interval of 6449 – 6537 m (88 m thickness) M-2. Based on these observations, we conclude that seismic inversion of the post-stack seismic data can be used as good indicator of lithology and pore fluid contrasts and to predict the presence of hydrocarbon accumulation in the porous gas and oil sands to reduce drilling risk.

**Keywords:** Hydrocarbon, Rock attributes, Lithology, seismic, reservoir

### 1. Introduction

Seismic amplitudes are usually observed on seismic sections due to contrasts in elastic rock properties at the interface between two geologic layers. Rock properties are those physical properties of a rock, which can affect the way seismic wave travel through the rock. They include P-wave velocity ( $V_p$ ), S-wave velocity ( $V_s$ ), density ( $\rho$ ), and their attributes (which are

---

✉ Samuel Ebong: [sirphysicsonline@gmail.com](mailto:sirphysicsonline@gmail.com)

Department of Physics (Geophysics Research Group), Akwa Ibom State University Mkpatt Enin, PMB 1162 Uyo, Nigeria

---

simple combination of the rock properties), P- and S- impedances ( $Z_p$  and  $Z_s$ ), Poisson's ratio ( $\nu$ ) and incompressibility ( $\lambda\rho$ ) and shear modulus ( $\mu\rho$ ) (Russell, *et al.*, 2003). Amplitudes can indicate layering as well as lateral variations in reservoir (Brown, 1997). Seismic amplitude analysis has been greatly employed in exploration, development, production and monitoring to provide deeper insight and understanding into the heterogeneity that exists in the subsurface, with particular interest in fluid and lithology discrimination and characterization. Seismic inversion, which involves calculating acoustic impedance (or velocity) from a seismic trace taken as representing the earth's reflectivity, is an essential first step to ensure proper

integration of seismic data, well logs, velocity information and geology. Any reservoir characterisation exercise usually begins with the available geological information and geophysical data. In this study, 3D seismic data is integrated with petrophysical well logs to discriminate fluids and lithology in the M field in the Niger Delta.

## 2. Location and Geology of the Study Area

Niger Delta Basin is situated at the southern end of Nigeria boarding the Atlantic Ocean where the M oil field is located. M oil field has several stacked reservoirs including the M-5000 reservoir analyzed in this study, which is 120.00 ft thick. The assumed wells are (M -1, 2 and 3) respectively as in Figure 1.

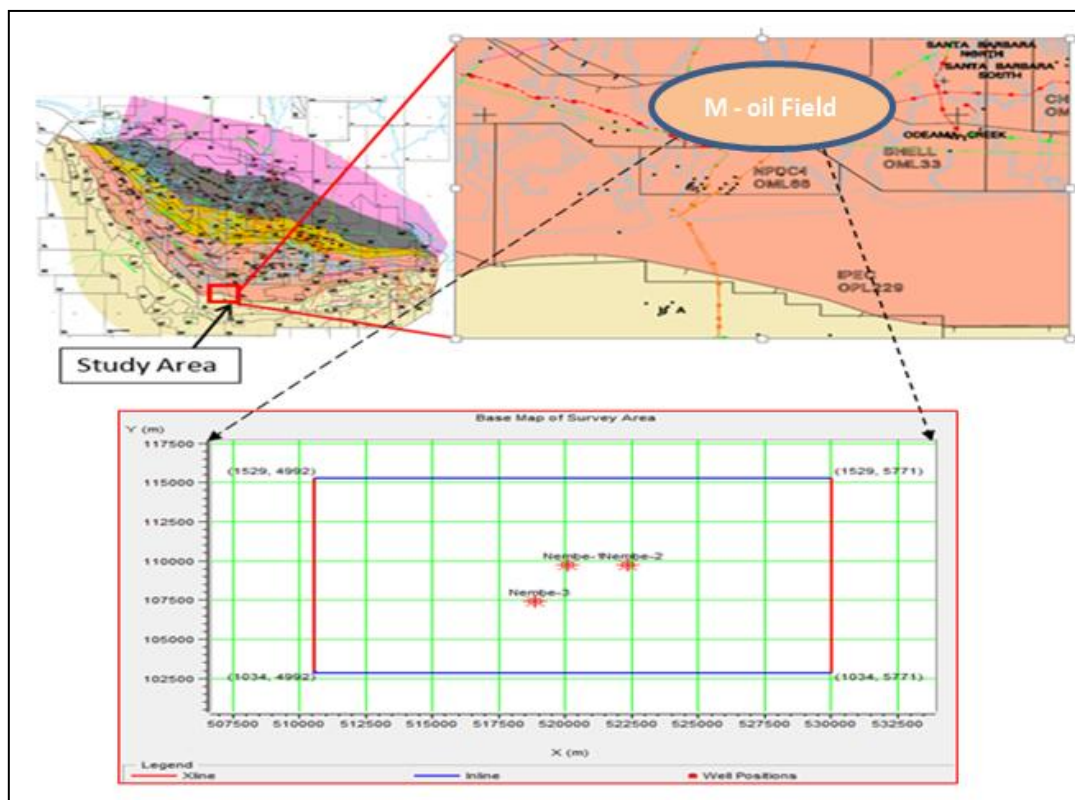


**Fig. 1:** location map showing the study area and Base Map

The Niger Delta Basin is situated along the southern end of Nigeria bordering the Atlantic Ocean between latitudes  $4^{\circ}\text{N}$  and  $8^{\circ}\text{N}$  and longitudes  $4^{\circ}\text{E}$  and  $6^{\circ}\text{E}$ . The onshore portion of the Niger Delta Province is delineated by the geology of southern Nigeria and south-western

Cameroon (Figure 2). The northern boundary is the Benin Flank-an east-northeast trending hinge line south of the West Africa Basement Massif. The north-eastern boundary is defined by outcrops of the Cretaceous on the Abakaliki High and further east-south-east by the Calabar

Flank a hinge line bordering the adjacent Precambrian (Doust and Omatsola 1990). The offshore boundary of the province is defined by the Cameroon Volcanic line to the east, the eastern boundary of the Dahomey Basin (the eastern-most West African transform-fault passive margin) to the west, and the two-

kilometer sediment thickness contour or the 4000-meter bathymetric contour in areas where sediment thickness is greater than two kilometers to the south and southwest. The province covers 300,000 km<sup>2</sup> and includes the geologic extent of the Tertiary Niger Delta (Akata-Agbada) Petroleum System.

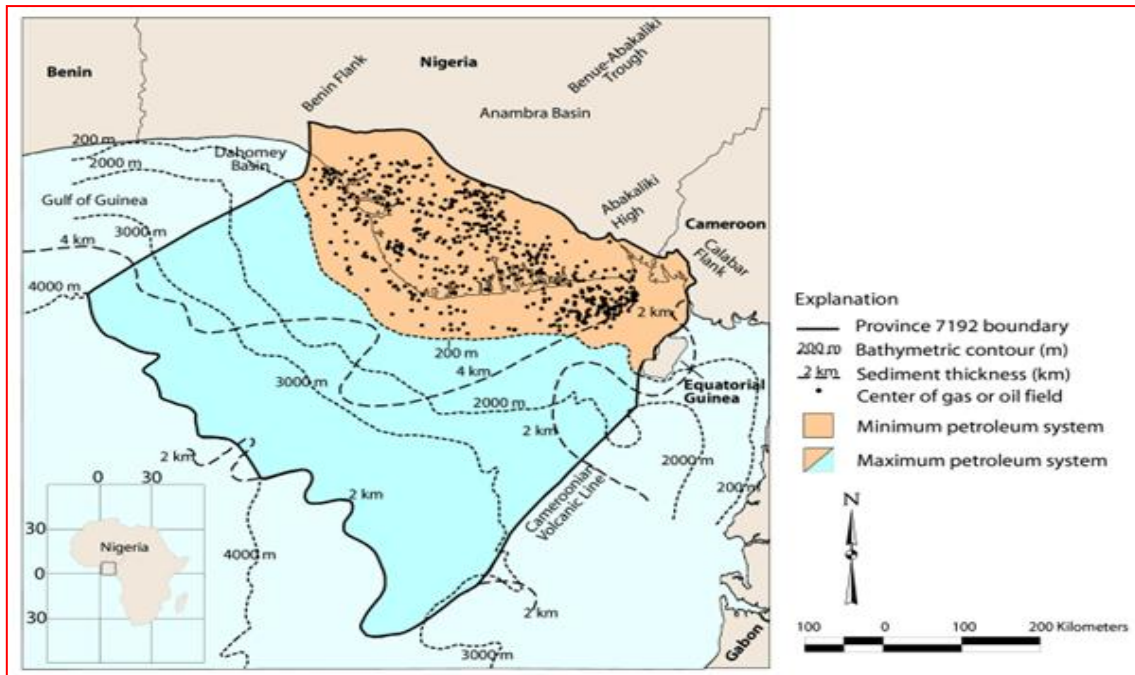


**Fig. 2:** Regional geology outline map of the Niger Delta (Tuttle *et al.*, 1999)

### 3. Theoretical Framework

Reservoir Characterization is a process of integrating various qualities and quantities of data in a consistent manner to describe reservoir properties of interest in inter well locations (Ezekwe and Filler, 2005). The main purpose of reservoir characterization is to generate a more representative geologic model of the reservoir properties. More so, the goal of any reservoir characterization or reservoir modelling is to understand the reservoir connectivity in static and dynamic conditions by integrating data from different sources (Kelkar and Perez, 2002).

**Statistical and Probabilistic Approach to Inversion:** Rothman's (1985) non-linear inversion, statistical mechanics, and residual

states estimation address the problem confronted in non-linear inversion when no good initial guess of the model parameters can be made. The non-linear inversion is set as a problem of Bayesian estimation, in which the prior probability distribution is the Gibb's distribution of statistical mechanics. The Gibbs-Markov model provides guidelines for the reduction of a large nonlinear inverse problem into small, independent and computationally manageable sub-problems that does not depend upon a good initial guess. The solution was obtained by maximizing the a-posterior probability of the model parameters. Optimization was performed with a Monte-Carlo technique-simulated annealing (SA). The result on residual statics estimation reveals that poorly picked correlations (cycle skips or leg

jumps) appear as local minima of the objective function, but that global optimization was successfully performed.

Tarantola (1986) proposed a reasonable strategy for non-linear inversion of real seismic reflection data with computers. The non-linear inverse problem is set as the problem of minimizing a (non-quadratic) function of the model parameters, essentially measuring the distance between observed and predicted data. The use of generalized least-squares criterion allows introduction of a priori constraints in which the vertical gradients of the model have to be small so that the resulting equations are very simple. The minimization problem was solved iteratively, using steepest descent (but suggested conjugate gradients also), by optimizing the P-wave impedance, the S-wave impedance and then the density in that order.

Nicolao *et al.* (1993) presented a simple linearized model, using Born approximation that allows a theoretical study of the effects of velocity errors in overburden. The observation was that the information contained in reflections and their retrieval can be achieved using singular value decomposition (SVD). The analysis was performed on two sets of elastic parameters ( $\Delta\alpha/\alpha$ ,  $\Delta\beta/\beta$ ,  $\Delta\rho/\rho$  and  $\Delta I_p/I_p, \Delta I_s/I_s, \Delta\rho/\rho$ ), and concluded that PP reflections allow estimation of only one linear combination of parameters (P-Impedance contrast) and the second linear combination (S-Impedance contrasts in the first approximation) upon the maximum incident angle and upon the velocity uncertainty in the overburden while estimation of the last parameter is very difficult. The result showed that a two-percent level velocity uncertainty could destroy information about the second combination of parameters.

Nevertheless, this study seeks to determine the application of rock physics theories for lithology and fluid characterization using inversion approach.

#### 4. Materials and Method

The methodology employed here examines the response of reservoir properties to the presence of hydrocarbons in M oil field. Next, to identify the rock properties that is more robust than others in terms of sensitivity to either fluid or lithology, or both. These more robust properties are extracted as volumes or slices using seismic inversion techniques and used in the identification and mapping of prospects. These attributes are computed from both well log and seismic data. At the end, the results from the three stages are analyzed in order to determine fluid presence and discriminate lithology in the reservoirs.

**Data Sets Used:** The data used in this work are well logs and seismic data from M oil field all in the coastal swamp depobelt within the Niger Delta basin. These data were analysed using Hampson Russell Software (HRS). The well log data were evaluated, also seismic and rock attribute cross-sections were created. Practically, check-shot correction was carried out in all wells.

**Post-Stack Seismic Inversion:** Seismic inversion is the procedure for extracting underlying models of the physical characteristics of rocks and fluids. Generally, it is used to estimate the physical properties of the rocks by combining seismic and well-log data. In many cases, the physical parameters of interest are the impedance, velocity and density. Attributes based on inversion are also utilized to improve the interpretation of seismic sections.

Usually, the inversion procedure depends on some form of forward modelling generating the earth response to a set of model parameters by using mathematical relationships. For example, we can produce a synthetic seismogram by using an elastic wave equation and a model with known parameters (velocity and density). For a known data set, the inversion consists in finding the model which reproduces the



observed data set. In addition, in the inversion method itself, multiple reflections, transmission loss, geometric spreading and frequency-dependent absorption are ignored. The common way to reducing these uncertainties is to use additional information (mostly from well logs), which contains low and high frequencies and constrains the deviations of the solution from the initial-guess model. The final result therefore relies on the seismic data as well as on this additional information, and also on the details of the inversion methods themselves.

**Model Based Inversion:** The model-based inversion depends on an initial low frequency P-impedance model, generated from well data and horizons based on the convolution model given in equation (1).

$$S = W * R + n \quad (1)$$

where  $S$  denotes the seismic trace,  $W$  is the wavelet,  $R$  is the reflectivity,  $n$  is the random noise, and “\*” denotes convolution in time. This method solves for the reflectivity iteratively, looking for differences between the real seismic trace and the synthetic trace formed from the model, and modifying the model to compensate the differences. The model-based inversion is a generalized linear inversion (GLI) algorithm which attempts to modify the model until the resulting derived synthetic matches the seismic trace within some acceptable bounds. For each trace, a synthetic seismogram was calculated using the initial impedance guess and the known wavelet. That impedance was then modified gradually, until the resulting synthetic trace matched the real trace within some tolerance level (Russell, *et al.*, 2003) After the low frequency scalar had been applied, the inversion was performed with the selection of the appropriate seismic volume (full segy in the field) and its corresponding impedance volumes and the bandwidth wavelet created. The processing time window was also selected as it allows us to invert the volume needed in order for noisy areas within the

volume not to overshadow the reservoir zone. The hard constrain option was chosen since this limits the amount of deviation of the inverted volume from the initial model.

## 5. Data Analysis, Result and Discussion

The result includes the identified reservoirs from logs, cross sections and horizon maps of rock attributes extracted from 3-D seismic data in M oil field. The corresponding cross section and horizon maps for some rock attributes were investigated in order to map out regions in the field that would account for probable presence of gas sands, oil sands or brine sands in the field of study.

**Well Log Analysis:** The well curves used for the analysis are well logs of M-1, M-2 and M-3; for M oil fields as shown in Figure 3a, b and c. The logs include gamma ray overlay with caliper log (except M-1 with no caliper), resistivity, density, P- wave, S-wave (only in M-1), Porosity and Water Saturation logs. The true vertical depth (TVD) of each well ranges from 5100 to 10000 m, 4900 m to 8000 m, and 4000 m to 9900 m, for M-1, M-2 and M-3 respectively. The reservoir of interest analyzed were M-5000 with thicknesses of 6450-6533m (M-1), 6449-6537m (M-2) and 6629-6711.67m (M-3) respectively. The three wells are shown in Figure 4. However, the wells exhibit a dominantly shale/sand/shale sequence typical of the Niger Delta formation. The wells were analysed in terms of fluid type and lithology within the zones of interest in which Shale lithologies were delineated by the high gamma ray (Shale lithologies cause the deflection of Gamma curve to the right) and resistivity to the far left due to its high conductive nature. Sand lithologies deflect the Gamma ray curve to the left and Resistivity curve to the far right indicating probable hydrocarbon charged sand. Thus, Regions showing low gamma ray, high resistivity, high porosities and low water saturation are mapped (circled) as sand lithologies with probable hydrocarbon zone in

each well as shown in Figure 3 above. On the other hand, regions showing high gamma ray, low resistivities, low porosities and high water saturation are mapped as shale lithologies.

**Seismic Inversion Attributes Analysis:** The goal of seismic inversion is to predict rock and fluid properties, for reservoir characterization from seismic data. It is difficult to identify fluids and lithologies from the P- and S-wave impedances ( $I_P$  and  $I_S$ ) alone because their values are not unique to different fluid-filled lithologies. If the lithology can be constrained, as is done above with well logs, we can concentrate on the fluids. Evaluation of information from the Lamé parameters ( $\mu\rho - \text{Mu-rho}$  and  $\lambda\rho - \text{lambda-rho}$ ) to further discriminate lithology/fluids contrast related to hydrocarbon charged sands and wet sands.

effectively reduce ambiguities in fluid and lithologic identifications that are based on only  $I_P$  and  $I_S$ . For reservoir characterization of M oil field with M-5000, we inverted the post stack seismic volumes of the oil field in Niger Delta to estimate the P-impedance ( $I_P$ ), S-impedance ( $I_S$ ),  $V_P/V_S$ , Lamé' parameters ( $\mu\rho - \text{Mu-rho}$  and  $\lambda\rho - \text{lambda-rho}$ ) to further discriminate lithology/fluids contrast related to hydrocarbon charged sands and wet sands.

**P- Impedance ( $I_P$ ) Cross-Section:** Figure 5 indicate the inverted P-impedance cross-section superimposed with 3D seismic volumes (Full Segy = full seismic exploration geophysics) from time window of 1800-2050 ms and 2100-2400ms.

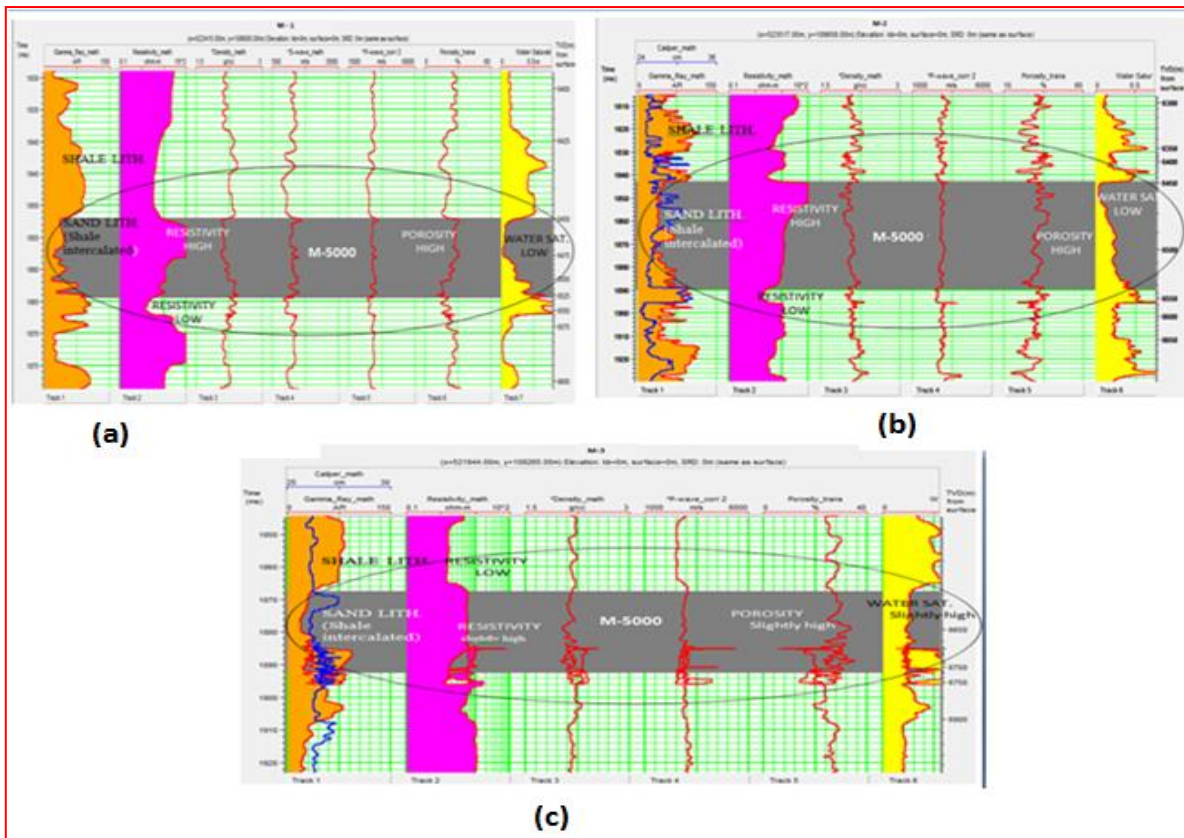


**Fig. 3:** (a) M-1 suite of logs used in the analysis; low-Gamma ray, high-Resistivity, low-Density, low-P-wave, little-increase S-wave, high-Porosity and low-Water Saturation with M- 5000 having a thickness of 6450 - 6533 m (83 m). (b) M-2 suite of logs used in the analysis; low-Gamma ray, high-Resistivity, low-Density, low-P-wave, high-Porosity and low-Water Saturation with M- 5000 having a thickness of 6449 - 6537 m (88m) (c) M-3 suite of logs used in the analysis; low-Gamma ray, slightly high-Resistivity, little-increased (Density, P-wave, Porosity and Water Saturation) with M- 5000 having a thickness of 6629-6711 m (82 m).

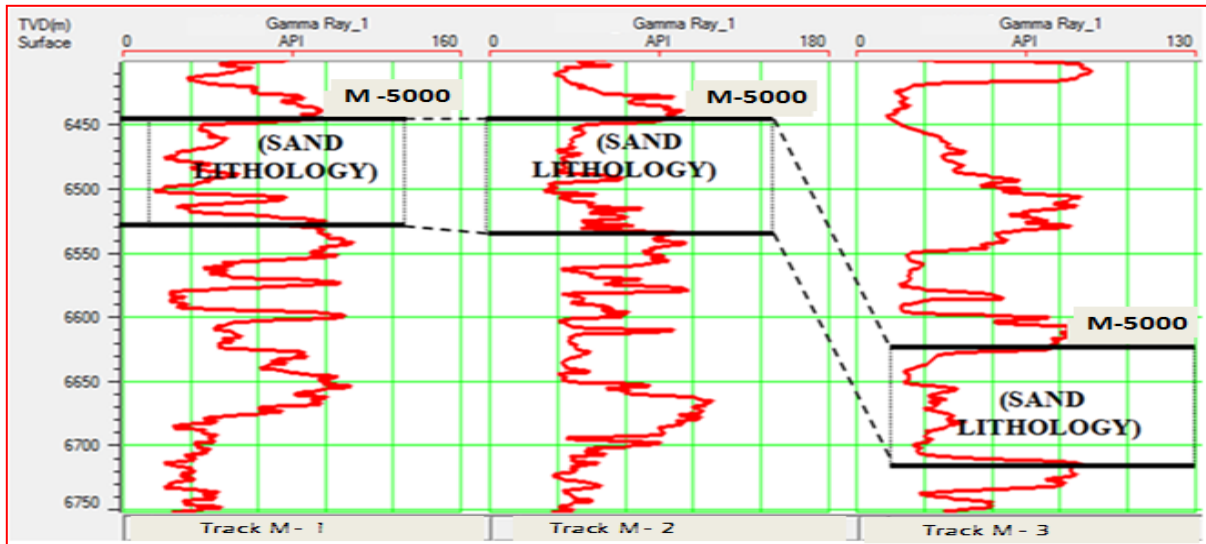


**Fig. 4:** Correlation of sand lithologies (M-5000) in M oil field using Gamma ray curves as guide

There is a good match between the  $I_p$  features distribution, seismic wiggles and the P-wave log (P-wave log is the black curve in the Inverted P-impedance cross section plotted at In-line and Xline: 1310, 5372; 1310, 5464; 1216, 5323; for M-1, M-2, M-3). In M oil field, the highest  $I_p$  values ( $2.4758 - 2.7899 \times 10^4 \text{ m/s} \times \text{g/cc}$ , blue and purple) correspond to M- shales. Intermediate acoustic impedance values ( $2.1168 - 2.4309 \times 10^4 \text{ m/s} \times \text{g/cc}$ , red and cyan) correspond to M- wet sands. The lowest  $I_p$  values ( $1.7129 - 2.0719 \times 10^4 \text{ m/s} \times \text{g/cc}$ , green and yellow) are associated with M oil field hydrocarbon charged sands. However, M- Horizon are indicative of the top of M-5000 reservoirs on inverted section, which show that these regions are bounded by low P-impedance due to hydrocarbon presence.

The horizontal time slice (amplitude map) – figure 5(d) extracted from P-impedance shows the hydrocarbon charge sands, wet sands and shales channels in which the highest  $I_p$  values ( $2.1029 - 2.2203 \times 10^4 \text{ m/s} \times \text{g/cc}$ , blue and purple) correspond to shales reflector, intermediate  $I_p$  values ( $1.9686 - 2.0861 \times 10^4 \text{ m/s} \times \text{g/cc}$ , red and cyan) correspond to wet sands reflector, and the lowest value of  $I_p$  ( $1.8176 - 1.9518 \times 10^4 \text{ m/s} \times \text{g/cc}$ ) correspond to hydrocarbon charged sand. Here the well

location exhibits low values of  $I_p$  especially in M-2 and M-3.

**$V_p/V_s$  Cross-Section:** Figure 6 shows the inverted  $V_p/V_s$  cross-section superimposed with 3D seismic volumes (Full Segy) from time window of 1800-2050 ms and 2100-2400ms. There is a good match between the  $V_p/V_s$  features distribution, seismic wiggles and the Gamma ray log (Gamma ray log is the black curve in the Inverted  $V_p/V_s$  cross section plotted at In-line and Xline: 1310, 5372; 1310, 5464; 1216, 5323 for M-1, M-2, M-3, respectively). The M oil field  $V_p/V_s$  section Figure 6 shows locally high values (2.48-2.78, blue and purple) that corresponding to M-shales, intermediate  $V_p/V_s$  values (2.11-2.44, red and cyan) corresponding to M- fluid (oil/brine), and locally low values (1.78-2.07, green and yellow) of  $V_p/V_s$  corresponding to Gas in the M oil field sandstone. However, M-Horizon are indicative of the top of M-5000 reservoirs on inverted section which show that these regions are bounded by low  $V_p/V_s$  due to hydrocarbon presence. The horizontal time slice (amplitude map) – figure 6(d) for M oil field extracted from  $V_p/V_s$  cross-section shows the Gas sandstone, wet sands and shales channels in which the highest  $V_p/V_s$  values (2.5047-2.7349, blue and purple) correspond to shales reflector, intermediate  $V_p/V_s$  values



(2.1593-2.4663, red and cyan) correspond to wet sands reflector, and the lowest values of  $V_P/V_S$  (1.8139-2.1209, green and yellow)

correspond to hydrocarbon charged sand. Here the well location exhibits low values of  $V_P/V_S$  especially in M-2 and M-3.

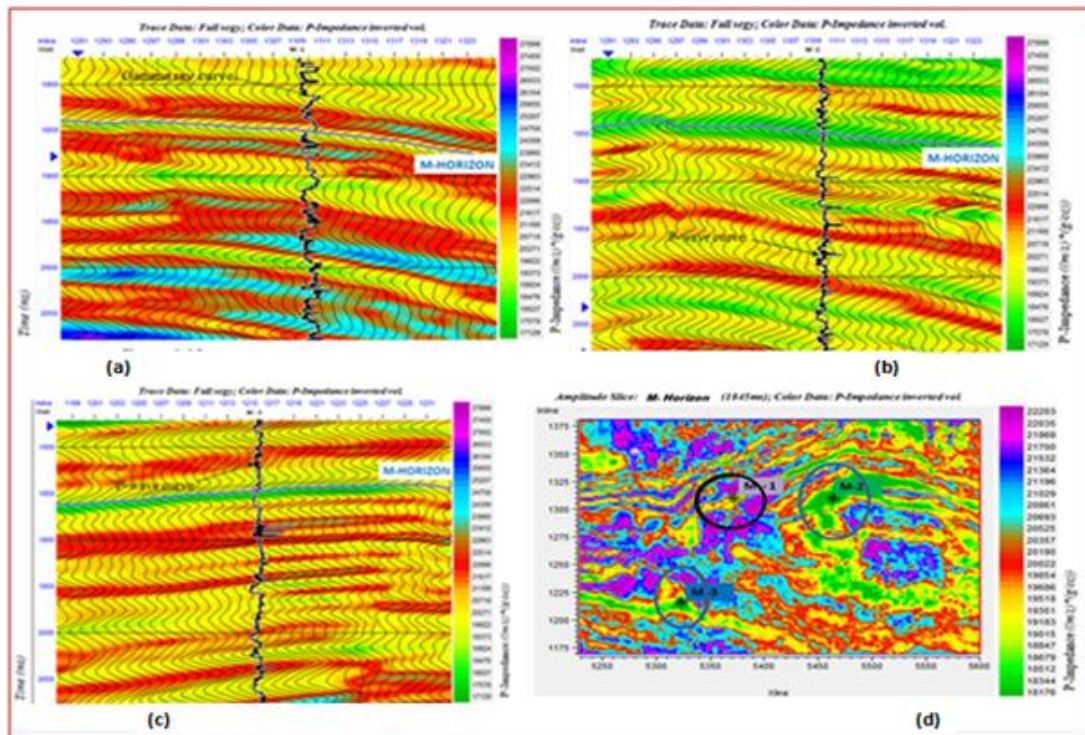


**Fig. 5:** M- oil field inverted  $I_p$  cross-section; (a) M-1 Plot, (b) M-2 plot (c) M-3 plot and (d) horizontal time slice (Amplitude map)

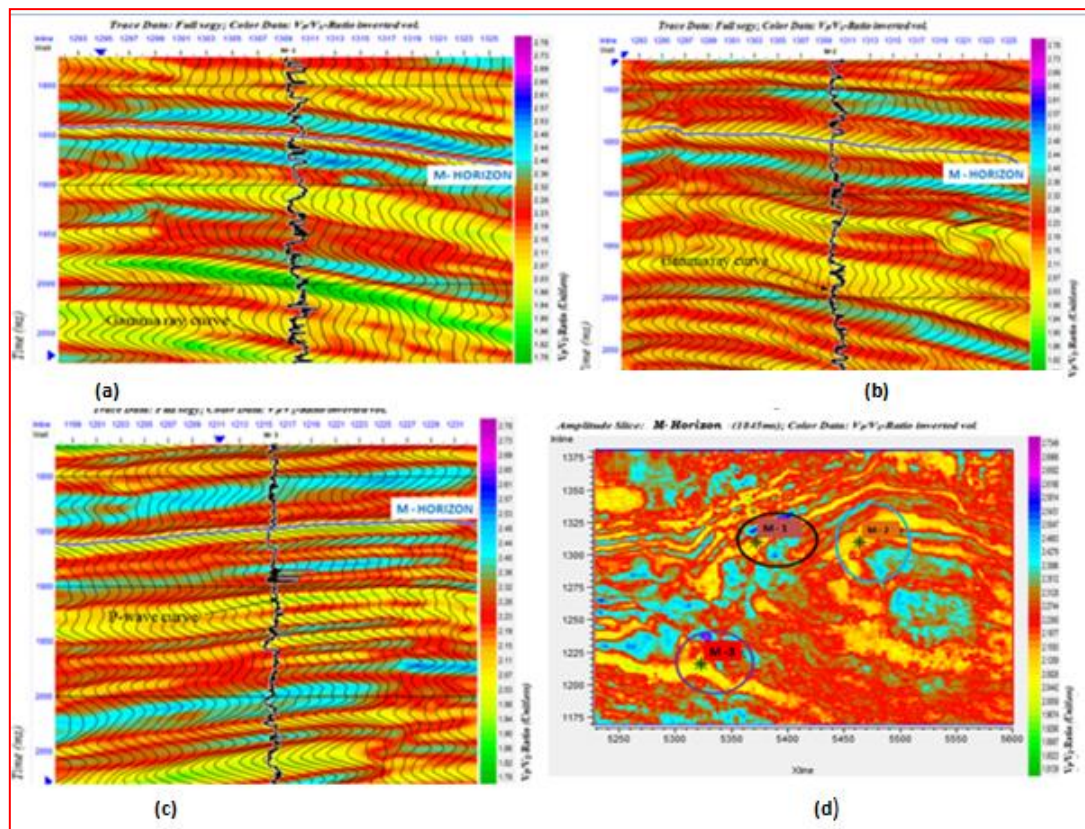


**Fig. 6:** M oil field inverted  $V_P/V_S$  cross-section; (a) M-1 Plot, (b) M-2 plot, (c) M-3 plot and (d) horizontal time slice (Amplitude map)



**S- Impedance ( $I_S$ ) Cross-Section:** Figure 7, M oil field shows the inverted S-impedance cross-section superimposed with 3D seismic volumes (Full Segy) from time window of 1800-2050 ms. There is a good match between the  $I_S$  features distribution, seismic wiggles and the P-wave log (P-wave log is the black curve in the Inverted P-impedance cross section plotted at In-line and Xline: 1310, 5372; 1310, 5464; 1216, 5323; for M-1, M-2, M-3 respectively). For M oil field, the highest  $I_S$  values ( $1.2456 - 1.4890 * 10^4 \text{ m/s} \times \text{g/cc}$ , blue and purple) correspond to M- shales. Intermediate Shear impedance values ( $8.807 * 10^3 - 1.2051 * 10^4 \text{ m/s} \times \text{g/cc}$ , red and cyan) correspond to M-wet sands. The lowest  $I_S$  values ( $5.157 - 8.401 * 10^3 \text{ m/s} \times \text{g/cc}$ , green and yellow) are associated with M oil field hydrocarbon

charged sands. However, M-Horizon is indicative of the top of M-5000 reservoir on inverted section which shows that these regions are bounded by low S-impedance due to hydrocarbon presence. The horizontal time slice (amplitude map) – figure 7(d) – for M- oil field extracted from S-impedance shows the hydrocarbon charge sands, wet sands and shales channels in which the highest  $I_S$  values ( $1.1377-1.3089 * 10^4 \text{ m/s} \times \text{g/cc}$ , blue and purple) correspond to shales reflector, intermediate  $I_S$  values ( $8.809 * 10^3-1.1092 * 10^4 \text{ m/s} \times \text{g/cc}$ , red and cyan) correspond to wet sands reflector, and the lowest value of  $I_S$  ( $6.242-8.524 * 10^3 \text{ m/s} \times \text{g/cc}$ ) correspond to hydrocarbon charged sand. Here the well location exhibits low values of  $I_S$  especially in M-2 and M-3.

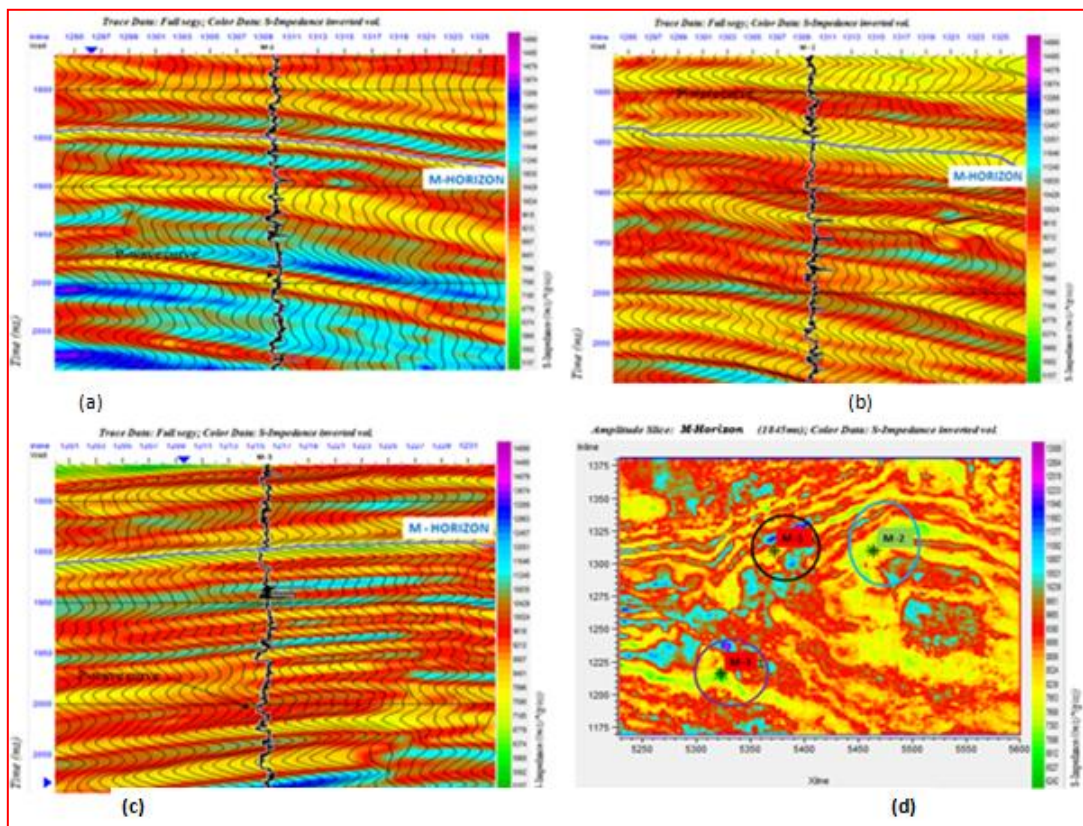


**Fig. 7:** M- oil field inverted  $I_S$  cross-section; (a) M-1 Plot, (b) M-2 plot, (c) M-3 plot and (d) horizontal time slice (Amplitude map)

**Lambda-Rho ( $\lambda\rho$ ) Cross section:** Goodway *et al.* (1997) shows that the Lamé's parameter terms  $\mu\rho$  and  $\lambda\rho$  are good pore fluid indicators

and can be calculated using equations (2) and (3).

$$\lambda\rho = I_P^2 - 2I_S^2 \quad (2)$$

$$\mu\lambda = I_S^2 \quad (3)$$

where the Lamé's parameters are  $\lambda$  (which is sensitive to pore fluid) and  $\mu$  (which is sensitive to matrix connectivity but is independent of the pore fluid) Dufour *et al.*,(2002).

Figure 8 shows the inverted Lambda-Rho ( $\lambda\rho$ ) cross-section superimposed with 3D seismic volumes (Full Segy) from time window of 1800-2050 ms. There is a good match between the  $\lambda\rho$  features distribution, seismic wiggles and the Gamma log (Gamma log is the black curve in the Inverted Lambda-Rho ( $\lambda\rho$ ) cross section plotted at In-line and Xline: 1310, 5372; 1310, 5464; 1216, 5323 for M-1, M-2, M-3). For M oil field, the highest  $\lambda\rho$  values (25.83 –

28.30 GPa \* g/cc, blue and purple) are indicative of shales. Intermediate  $\lambda\rho$  values (23.02 – 25.43 GPa \* g/cc, red and cyan) are indicative of oil/brine. The lowest  $\lambda\rho$  values (19.85 – 22.67 GPa \* g/cc, green and yellow) are indicative of Gas. The horizontal time slice (amplitude map) – Figure 8(d) extracted from  $\lambda\rho$  cross-section shows the hydrocarbon charge sands, wet sands and shales channels in which the highest  $\lambda\rho$  values (24.38-27.23 GPa x g/cc, blue and purple) are indicative of shales reflector, intermediate  $\lambda\rho$  values (21.13-23.97 GPa x g/cc, red and cyan) are indicative of oil/brine sands reflector, and the lowest value of  $\lambda\rho$  (17.46-20.72 GPa x g/cc) are indicative of hydrocarbon (Gas) charged sand. Here the well location exhibits low values of  $\lambda\rho$  especially in M-2 and high values of  $\lambda\rho$  in M-1 and M-3.

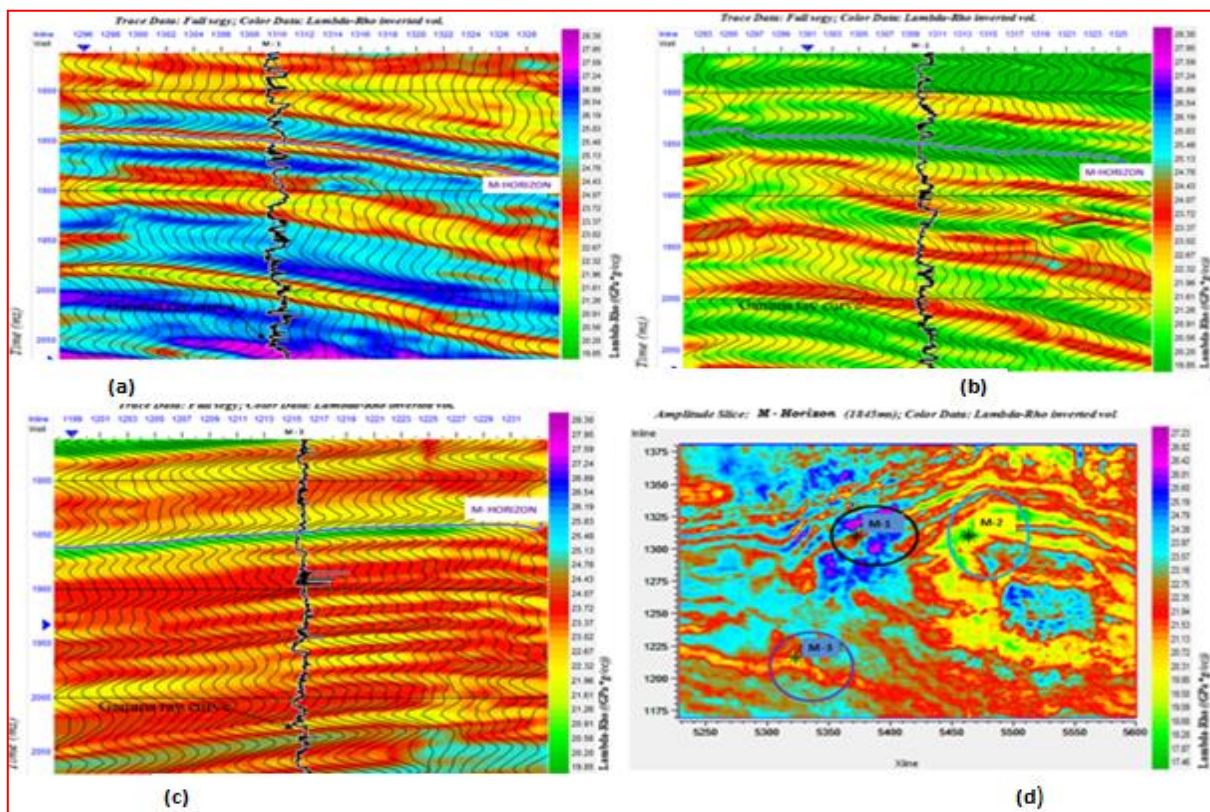


**Fig. 8:** M oil field inverted Lambda-Rho ( $\lambda\rho$ ) cross-section (a) M-1 Plot, (b) M-2 plot, (c) M-3 plot and (d) horizontal time slice (Amplitude map)

**Mu-Rho ( $\mu\rho$ ) Cross-section:** The Mu-rho attribute gives a quantitative measure of the variation in rigidity and lithology (Goodway et al., 1997). Figure 9 for M oil field indicate the

inverted Mu-Rho ( $\mu\rho$ ) cross-section superimposed with 3D seismic volumes (Full Segy) from time window of 1800-2050 ms. There is a good match between the  $\mu\rho$  features



distribution, seismic wiggles and the Gamma log (Gamma log is the black curve in the Inverted Lambda-Rho ( $\mu\rho$ ) cross section plotted at In-line and Xline: 1310, 5372; 1310, 5464; 1216, 5323 for M-1, M-2, M-3 respectively).

For M oil field, the  $\mu\rho$  is a lithology indicator with high values (14.2 – 18.2 GPa \* g/cc, blue and purple) indicative of Shales. Intermediate  $\mu\rho$  values (9.7 – 13.7 GPa \* g/cc, red and cyan) indicative of wet sands. The lowest  $\mu\rho$  values (4.6 – 9.1 GPa \* g/cc, green and yellow) indicative of Gas sand saturation. The horizontal time slice (amplitude map) – figure

9(d) – for M oil field extracted from  $\mu\rho$  cross-section shows the hydrocarbon charge sands, wet sands and shales channels in which the highest  $\mu\rho$  values (12.3-15.9 GPa x g/cc, blue and purple) are indicative of shales reflector, intermediate  $\mu\rho$  values (8.2-11.8 GPa x g/cc, red and cyan) indicative of oil/brine sands reflector, and the lowest value of  $\mu\rho$  (3.6-7.7 GPa x g/cc) indicative of hydrocarbon (Gas) charged sand. Here the well location exhibits low values of  $\mu\rho$  especially in M-1, M-2 and M-3

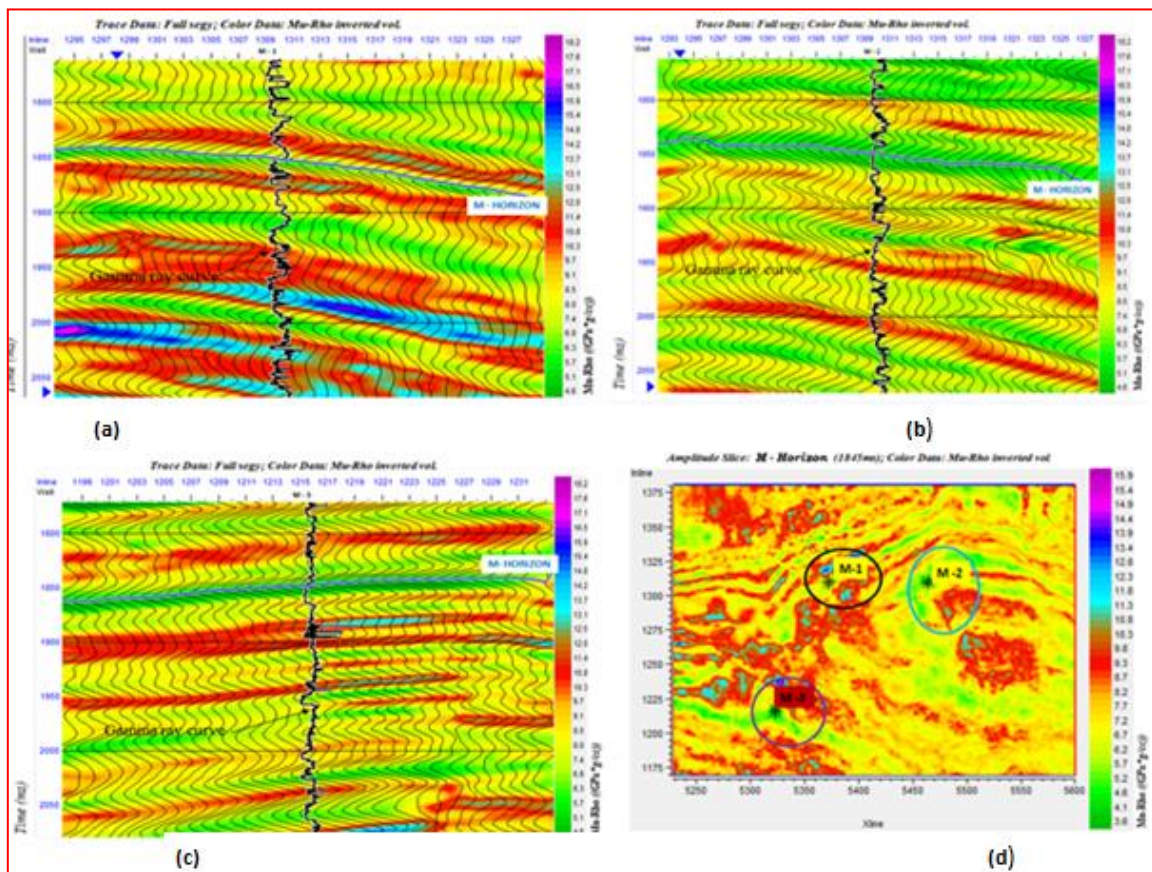


**Fig. 9:** M oil field inverted Mu-Rho ( $\mu\rho$ ) Cross-section; (a) M-1 Plot, (b) M-2 plot, (c) M-3 plot and (d) horizontal time slice (Amplitude map)

Five well attributes have been combined in all the three wells in the M oil field within M-5000 reservoirs. The P-impedance ( $I_P$ ),  $V_P/V_S$ , and the lames' parameters ( $\mu\rho$ ,  $\lambda\rho$ ) were found to be most robust in lithology and fluid discrimination within the reservoirs. Inversion of 3D post stack seismic data was performed to directly generate acoustic impedance volumes

from which rock attributes and petrophysical properties ( $V_P/V_S$ ,  $I_P$ ,  $I_S$ ,  $\lambda\rho$  and  $\mu\rho$ ) were extracted from seismic volumes for comparison in the well log analysis. The P-wave/Gamma ray curve is bounded by the top of M-5000 on inverted volumes with the lowest values of  $V_P/V_S$ -Ratio (1.9290),  $I_P$  (18176),  $\lambda\rho$  (6.7), and  $\mu\rho$  (18.68). Table 1 indicate hydrocarbon (gas)



charged sands. Also the high values of all these parameters might be due to shales/wet sands intercalations.

**Table 1:** Showing wells locations in horizontal time slices (Amplitude Maps) of each inverted volume of seismic attributes

Wells	$I_P$ (m/s*g/cc)	$I_S$ (m/s*g/cc)	$V_P/V_S$ (Unitless)	$M\rho$ (GPa*g/cc)	$\lambda\rho$ (GPa*g/cc)
M-1	19518	8239	2.1593	21.94	6.7
M-2	18176	7098	1.9290	18.68	3.0
M-3	18847	7668	1.9674	21.13	4.1

## 6. Conclusion

Acoustic impedance inversion of a 3D data set from the M oil field was investigated, to image the field subsurface to detect the hydrocarbon accumulation using M-5000 with integration of three wells from the field (M-1, M-2, and M-3). The well and seismic tie reveals that the hydrocarbon charged sands (gas sands -M-2, M-5000) are associated with low values of seismic attributes on the inverted cross-section and wet/shales, which could be possible seal or source rock associated with M-3 well having increase in extracted seismic attributes.

Analysis of all acoustic impedance parameters suggest that in M oil field (figures 5(b) - 9(b) and Table 1); the P-wave/Gamma ray curve is bounded by at the top of M-5000 on inverted volumes with the lowest values of  $V_P/V_S$  (1.9290),  $I_P$  (18176),  $\lambda\rho$  (6.7), and  $\mu\rho$  (18.68). This indicates hydrocarbon (gas) charged sands. Also the high value of all these parameters might be due to shales/wet sands intercalations. However, results from  $\lambda$ - $\mu$ - $\rho$  inversion provided greater insight into rock properties for pore fluid and lithology discrimination by isolating Lamé's impedance parameters (Lambda-Rho ( $\lambda\rho$ ) and Mu-Rho ( $\mu\rho$ )) from the seismic reflectivity response.

The combined interpretation of  $V_P/V_S$ ,  $I_P$ ,  $I_S$ , Lambda-Rho ( $\lambda\rho$ ) and Mu-Rho ( $\mu\rho$ ) attributes from the post-stack 3D seismic data enhanced the identification and delineation of

hydrocarbon charged sands with greater confidence. Low values of Lambda-Rho ( $\lambda\rho$ ),  $V_P/V_S$ ,  $I_P$ , associated with moderate to high values of Mu-Rho ( $\mu\rho$ ), indicate the presence of hydrocarbons within the sand reservoirs (M-5000). These results demonstrates that our approach can be applied with confidence in delineating hydrocarbons sands in mature field within the Niger Delta Basin and thereby increasing production from such field.

## References

- Brown, A., (1997). Porosity variation in carbonates as a function of depth: Mississippian Madison Group, Williston Basin, in J.A. Kupecz, J. Gluyas, and S.Bloch, eds., Reservoir quality prediction in sandstones and carbonates: AAPG Memoir 69, p. 29-46.
- Dufour, J., J. Squires, W. N. Goodway, A. Edmunds, and I. Shook, (2002). Integrated Geological and Geophysical interpretation case Study and Lamé Rock Parameter Extractions using AVO analysis on the Blackfoot 3C-3D seismic data, southern Alberta, Canada: Geophysics, **67**, 27-37.
- Doust, H., and Omatsola, E., (1990). Niger Delta, in, Edwards, J. D., and Santogrossi, P.A., eds., Divergent/passive Margin Basins, AAPG Memoir

- 48: Tulsa, American Association of Petroleum Geologists, p. 239-248.
- Ezekwe, J. N and Filler, S. L (2005). Modeling Deepwater Reservoirs, Paper presented at the SPE Annual Technical Conference and Exhibition, Dallas, Texas, October 2005. Paper Number: SPE-95066 - MS, <https://doi.org/10.21-18/95066-MS>
- Goodway, B., Chen, T. and Downton, J. (1997). Improved AVO fluid detection and lithology discrimination using Lamé petrophysical parameters; ' $\lambda\rho'$ ', ' $\mu\rho'$ ', & ' $\lambda/\mu$  fluid stack' from P and S inversions: 67th Annual International Meeting, SEG, Expanded Abstracts, 183-186.
- Kelkar, M. and Perez, G. (2002). Applied Geostatistics for Reservoir Characterization, SPE, Dallas, TX (2002). International Journal of Innovative Research in Science, Engineering and Technology *Vol. 2, Issue 4*.
- Li, Y. Y., and Downton, J. (2000). Application of amplitude versus offset in carbonate Reservoirs: Re-examining the potential: 70th Annual International Meeting, SEG, Expanded Abstracts, 166 –169.
- Nicolao, A., Durufuca, G., and Rocca, F., (1993). Eigenvalues and Eigenvectors of Linearized elastic inversion: Geophysics, 58, 670 -679. Niger Delta: American Association of Petroleum Geologists.
- Rothman, D. H., (1985). Nonlinear inversion, statistical mechanics and residual statics estimation: Geophysics, 50, 2784 - 2796.
- Russell, B. H., Hedlin, K., Flilerman, F. J., and Lines, L.R., (2003). Fluid-property discrimination with AVO: A Biot-Gassmann perspective: Geophysics, 68, 29-39.
- Tarantola, A., (1986): A strategy for nonlinear elastic inversion of seismic data: Geophysics, 51, 1893 - 1903.
- Tuttle, M. L. W., Charpentier, R. R. and Brownfield, M. E. (1999). The Niger Delta petroleum system: Niger Delta province, Cameroon, and Equatorial Guinea, Africa: <http://greenwood.cr.usgs.gov/energy/Won dEnergy/O F99-50H/ChapterA.htm#TOP>